Theor Chem Acc (2014) 133:1575
DOI 10.1007/s00214-014-1575-5

REGULAR ARTICLE

Quantum molecular dynamics simulations of liquid benzene using orbital optimization

Nazar Ileri · Laurence E. Fried

Received: 22 April 2014 / Accepted: 26 August 2014 / Published online: 25 September 2014

Abstract The structure of liquid benzene is investigated by quantum molecular dynamics simulations. Results using variationally optimized numerical pseudo-atomic orbitals are compared to those of generic optimized orbitals. The accuracy of the first-principle calculations is compared with recent experimental findings. Simulations using minimal basis sets with optimized orbitals are shown to successfully predict the local structure of liquid benzene, while simulations with non-optimized minimal basis sets have significant errors in the structure of the first solvation shell. The use of a minimal optimized basis set considerably speeds up simulations, while preserving much of the accuracy of a larger basis set formed by generic orbitals. The transferability of the optimized orbitals is also explored under different environmental conditions.

Keywords Liquid benzene · Ab initio simulations · Orbital optimization · Krylov · Direct diagonalization

1 Introduction

Benzene is an important organic solvent that finds uses in many industrial and scientific applications. It is the simplest aromatic hydrocarbon, constituting the building blocks of many important complex molecules. Furthermore, it provides an important example of aromatic π–π interactions, which have been of great interest to numerous fields including crystal packing [1], drug design [2], molecular recognition [3], and DNA/RNA base stacking [4]. Due to the aromatic π-bonding and electron delocalization, benzene has exceptional stability at ambient conditions.

Detailed knowledge of the structural properties of benzene is necessary for better understanding of π-interactions in condensed matter. Solid state benzene is well-known to have a herringbone pattern [5–7]. The structure of an isolated benzene dimer in the gas phase [8–16] has also received much attention; both experimental and theoretical results indicate almost isoenergetic, parallel displaced, and T-shaped configurations. The T-shaped configuration is accepted as the true global energy minimum today [12, 17–19]. Benzene in the liquid state, however, is less well understood. Theoretical [20] and experimental studies by X-ray diffraction [21–23] and neutron diffraction [24–27] techniques on the structure of liquid benzene have shown that the local ordering in liquid benzene is mostly perpendicular L-shaped [21, 22, 24] and/or T-shaped [23, 26, 27]. More recently, a parallel displaced and a perpendicular Y-shaped arrangement have been proposed [25] at separations <0.5 and >0.5 nm, respectively, by high-resolution neutron diffraction experiments supported with empirical potential structure refinement analysis. In addition, the perpendicular T-shaped configuration is reported to occur only as a saddle point in the liquid state [25].

Due to the lack of conclusive experimental data, numerous computational studies have been performed to shed light on the structural properties of liquid benzene. In particular, a number of studies have employed the molecular dynamics (MD) [28–30] and Monte Carlo (MC) [31, 32] techniques with empirical force fields. However, results obtained greatly depend on the force fields used. Conventional atom-centered force fields generally predict random

Dedicated to Professor Greg Ezra and published as part of the special collection of articles celebrating his 60th birthday.

N. Ileri · L. E. Fried (✉)
Physical and Life Sciences Directorate, Lawrence Livermore National Laboratory, Livermore, CA 94550, USA
e-mail: fried1@llnl.gov

or slightly favor perpendicular orientations [25, 33, 34]. A charge-separated all-atom force field [31] based on the Hunter and Sanders model [35], where a charge distribution above and below the aromatic ring represents the π-electrons, has resulted in perpendicular configurations being strongly preferred [31, 36, 37]. Recently, Fu and Tian [28] have compared different force fields and concluded that separation of charges or fitting the ab initio pairwise potentials does not necessarily guarantee the reliability of the force fields. They obtained the best fit to the latest experimental results [25] with the optimized potentials for liquid simulations (OPLS-AA) force field.

Density functional theory (DFT)-based ab initio MD simulations have been widely used to study the structural properties of ionic liquids, which often contain complex ring structures [38–40]. It has also been shown to provide an accurate description of π-aromatic interactions in benzene [14, 41, 42]. However, DFT–MD simulations scale poorly with computational effort and hence are practically limited to relatively small system sizes (several hundred atoms) and very short time periods (<10 ps). Liquid state simulations present particular challenges, due to the possibility of slow equilibration times and significant system size effects. Therefore, structural studies of benzene by DFT–MD simulations have mostly focused on the benzene dimer and small benzene clusters [41, 43–45]. Only recently, phase changes in solid benzene at pressures up to 300 GPa [46] as well as in shock-compressed liquid benzene (up to 70 GPa) [47] have been investigated by DFT–MD, which has been proven to be particularly suitable for the study of the chemical reactions in condensed and gas phases [48, 49].

First-principles DFT calculations generally scale as the third power of the number of atoms present in the simulation cell. Therefore, simulations of large and complex systems by DFT–MD necessitate the use of linear-scaling methods (O(N)), where the computations scale only linearly with the system size. Variationally optimized numerical atomic orbitals, which we will refer to as optimized atomic orbitals (OAO), have been shown to provide efficient and accurate localized orbitals as a basis set, suitable for linear-scaling methods [50–53]. OAO have been well documented and successfully employed in the simulation studies of isolated molecules and biomolecules [51, 54] as well as solids [51, 55], but there are few examples for neat molecular liquids. Recently, liquid water simulations [53] have been performed using improved polarization orbitals with a screened Coulomb confinement potential developed for water-based systems [52]. In addition, solid–liquid interface simulations of an electrochemical system containing propylene carbonate have been conducted by combining effective-screening medium method with O(N) DFT [55].

To this end, here, we study the structure of liquid benzene by ab initio MD simulations. This approach avoids the many adjustable parameters involved with empirical force fields, while allowing for the possibility of chemical reaction at extreme temperatures and pressures. Numerical atomic orbitals are variationally optimized specifically for benzene, based on the force theorem. The benzene-specific optimized orbitals are used as a basis set in comparison with generic orbitals. The generic orbitals are optimized from pseudo-atomic orbitals across a wide range of chemical conditions. The transferability of the OAO is tested under different environmental conditions. Effects of long-range interatomic London dispersion interactions are investigated. We show that orbital optimization considerably improves the calculations of a molecular liquid with a fixed basis set. The simulations with a minimal optimized basis set are substantially faster than those of a larger basis set formed by generic orbitals, yet retain much of the accuracy of the larger basis.

2 Computational details

The initial configuration of liquid benzene was obtained by MD simulations using OPLS-AA empirical force field [56, 57] as implemented in the GROMACS software package [58, 59]. Procedures were based on the simulations conducted by Fu et al. [28]. Ten benzene molecules were generated in a cubic simulation box of size 1.484 nm^3 with periodic boundary conditions, setting the density equal to the experimental value [60]. The system was energy minimized for 5,000 steps using the conjugate gradient minimization algorithm, with one steepest descent step for every ten conjugate gradient steps. Then, the equilibration and production runs were performed at 300 K temperature and 1 atm pressure in an NPT ensemble, each for 10 ns and with a time step of 1 fs. The temperature and pressure of the system were controlled by a Nose–Hoover thermostat [61, 62] and a Parrinello–Rahman isotropic barostat [63, 64] with a coupling time of 0.5 and 2.0 ps, respectively. A 0.5-nm cutoff distance was applied for Van der Waals interactions with a long-range dispersion correction for energy. Coulomb interactions were calculated by the particle-mesh Ewald (PME) method using a 0.5-nm cutoff for real space, a 0.12-nm grid spacing, and a PME order of 8. All bonds were constrained with the P-LINCS algorithm [65, 66]. A final density of 861 kg/m^3 was achieved in the production run, which is in good agreement with the experimental value of 876.5 kg/m^3.

Ab initio MD simulations of benzene were performed using the OpenMX software package [50, 51, 54, 67, 68], based on Kohn–Sham DFT [69], and basis set consisting of a linear combination of localized pseudo-atomic

orbitals. The Perdew–Bruke–Ernzerhof (PBE) exchange–correlation functional [70] within the generalized gradient approximation was adopted. Norm-conserving pseudopotentials proposed by Morrison et al. [71] are employed. The pseudo-atomic orbitals, generated by a confinement potential scheme [50, 51, 54, 67], had a cutoff radius of 5.0 a.u (except for calculations referred to below as PBE/DZP-7, where the cutoff radius was set to 7.0 a.u) for both hydrogen and carbon atoms. In principle, the complete basis set limit is approached as both the number of orbitals per atom and the cutoff radius are increased. For each element, single valence (commonly referred to as single zeta or SZ), double valence plus single polarization (DZP), and triple valence plus single polarization orbitals (TZP)-(H:s3p1, C:s3p3d1) as well as optimized contracted single valence orbitals (H:s1, C:s1p1) obtained from the generic (H:s6, C:s6p6) basis set; generic orbitals are the optimized pseudo-atomic orbitals provided by OpenMX) produced by the orbital optimization method [50, 51, 54] were used for the basis set. The DFT-D2 method [72] was employed to include the Van der Waals interaction. For orbital optimization, atomic basis orbitals with the same element type were optimized using the same orbital. The maximum number of self-consistent field iterations and the self-consistence field convergence criterion were 100 and 10^{-4} (Hartree/bohr)^2, respectively.

For calculations using optimized orbitals, a system size of 80 benzene molecules were also studied by replicating fully equilibrated configurations of ten molecules in three dimensions. The starting configurations were achieved through the same basis set as the one employed in larger system size. The real-space grid technique [73] was used to calculate the Hamiltonian matrix elements within an accuracy of 10^{-6} Hartree. A cutoff energy of 150 Ry was chosen in the numerical integrations and in the solution of Poisson's equation using the fast Fourier transformation algorithm (FFT). Unlike the small system size (10 benzene molecules) where the direct diagonalization method was used, large system calculations employed the linear-scaling Krylov subspace method [74] with the radius of a sphere centered on each atom and the dimension of the Krylov subspace set to 0.5 nm and 400, respectively. The radius of 0.5 nm was selected among the investigated parameters of 0.5, 0.6, 0.7 nm, since the simulations were faster and the results were only slightly different from those with a larger sphere radius. The dimension of the Krylov subspace, on the other hand, was set to the default value of the software. A cubic periodic boundary simulation cell was used and the MD time step was set to 0.5 fs, in all simulations. Three different temperature and density conditions were studied as follows: (300 K, 861 kg/m^3), (573 K, 570 kg/m^3), and (814 K, 1,400 kg/m^3). The electron and ion temperatures were set equal in order to achieve local thermodynamic

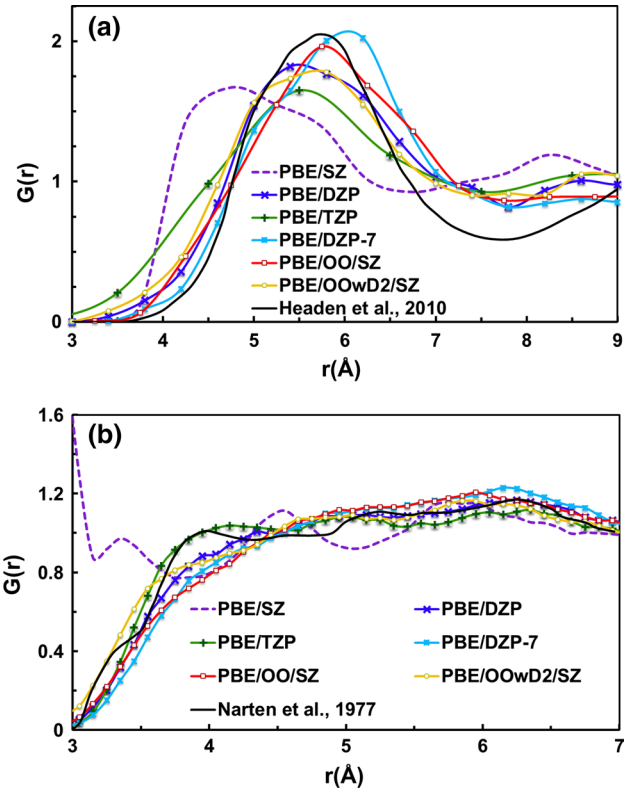

Fig. 1 RDFs of **a** the COM of benzene molecules, **b** C–C atom pairs. Experimental data cited from **a** Ref. [25] and **b** ref [22]. The best fits to experimental results are obtained with **a** PBE/OO/SZ and **c** PBE/TZP

equilibrium. All geometries were optimized by the steepest descent algorithm until the forces were $<10^{-4}$ a.u. Equilibration runs were performed in an NVT ensemble by scaling the velocities [75] for 2 ps and subsequently by the Nose–Hoover method [61, 62, 76] for 8 ps. The mass of heat bath for the Nose–Hoover thermostat was set to 100 a.u. Properties were calculated using the data from the final 8 ps Nose–Hoover MD runs after the equilibrium is achieved.

3 Results and discussion

The radial distribution functions (RDFs) of the center of mass (COM) of benzene molecules as well as the C atoms pairs for the ten molecule system are given in Fig. 1. The COM-RDFs provide general information on the size and number of molecules within the first solvation shell (Fig. 1a). It has been calculated by the relation $G(r) = V/N^2 \sum_{i<j} \delta(r - r_{ij})$ and compared to the experimental findings reported by Headen et al. [25]. Computations with the optimized single valence orbitals (PBE/OO/SZ) have predicted the best $G(r)$ values when compared to

experiment. A coordination number of approximately 12 in the first solvation shell is obtained with all calculations in agreement with the experimental value, except for the single valence orbitals (PBE/SZ) where only nine nearest neighbors are found. Similarly, the differences in the peak positions are calculated to be within 0.3 Å, excluding PBE/SZ where the difference is ~1 Å. The best peak positions are attained with the optimized single valence orbitals with and without the DFT-D2 method (PBE/OOwD2/SZ and PBE/OO/SZ respectively). In contrast, the best fit to the first minimum outside of the first shell is achieved through double valence orbitals with polarization (PBE/DZP and PBE/DZP-7) as well as PBE/OO/SZ. The difference in the first minimum compared to the experimental value is less than 0.3 Å with PBE/OO/SZ, PBE/DZP-7, and PBE/TZP. Similar to COM-RDFs, C atom pair RDFs (Fig. 1b) provide overall features of liquid structure obtained through different basis sets, but in greater detail. Besides, experimental C atom pair RDFs are generally easier to measure and more accurate compared to the COM-RDFs, which is a weighted average of C–C, C–H, and H–H RDFs [26]. All triple and double valence orbitals with polarization (PBE/DZP-7, PBE/TZP, and PBE/DZP) predict the first three peaks of the RDF (the peak positions were reported as 4.0, 5.2, and 6.3 Å by Narten et al. [21, 22]) within 0.3 Å deviation. The best first peak estimate is obtained with PBE/TZP at 4.1 Å, while the best second and third peak estimates are achieved at about 5.2 Å with PBE/DZP and PBE/DZP-7 and at 6.3 Å with PBE/DZP, respectively. In general, PBE/TZP calculations have resulted in the best intensity profile, while PBE/SZ has yielded in the worst profile as well as the peak positions, which are observed at r values more than 0.5 Å before reported values. This is indicative of a large effective attraction between neighboring benzene molecules, perhaps produced by basis set superposition error. Unlike generic single zeta orbitals (PBE/SZ), optimized single zeta orbitals (both PBE/OO/SZ and PBE/OOwD2/SZ) provide satisfying results, although they fail to locate the first peak of the C–C RDFs. Particularly, the intensity results of PBE/OOwD2/SZ are in good agreement with both PBE/DZP and PBE/TZP computations. The second and the third peaks are found to be at 5.0 and 6.0 Å with PBE/OO/SZ, and at 5.1 and 6.0 Å with PBE/OOwD2/SZ, respectively.

The simulated structure of liquid benzene is further investigated by the radial-angular pair distribution function (RADF), which gives some information on the degree of orientational order [25, 29, 30] (Fig. 2). The RADF has been computed for the minimum angles between the normals of aromatic planes using the equation $g(r,\theta) = 1/N\rho 4\pi r^2 \sin\theta \Delta r \Delta\theta \ [\Sigma_i \Sigma_{i\neq j} \delta(r - r_{ij}) \delta(\theta - \theta_{ij})]$, where ρ is the bulk number density, Δr and $\Delta\theta$ are the radial and angular resolution. In accordance with the experimental and computational findings [22, 23, 25, 28, 31], PBE/DZP-7, PBE/SZ, PBE/OOwD2/SZ, and PBE/OO/SZ calculations show a preference for perpendicular ordering in the first shell with the highest $g(r,\theta)$ values at $\theta \sim 90°$. The main peaks are obtained at 5.8, 4.8, 5.3, and 5.8 Å, respectively. Similar to Headen's findings [25] a shoulder is observed at $r \sim 4$ Å at low angles with PBE/DZP-7, PBE/OO/SZ, and PBE/OOwD2/SZ (Fig. 2d–f), indicating the existence of a parallel molecular arrangement at small molecular separations. On the other hand, the first peaks are shifted to $r \sim 4$ Å at $\theta < 20°$, with PBE/DZP and PBE/TZP calculations (Fig. 2b, c) while they remain at 5.8 and 5.3 Å, respectively, at $\theta > 20°$. Indeed, the peak values estimated for PBE/DZP and PBE/TZP at $r \sim 4$ Å and $\theta < 20°$ are much greater than the values obtained at $\theta \sim 90°$, showing higher preference for parallel ordering with increasing basis set size. Analysis of the simulation trajectories has revealed that Y-shaped and distorted L-shaped configurations with separation distances $r > 0.5$ nm (Fig. 3a) are the predominant geometry throughout the simulation time with PBE/DZP-7, PBE/SZ, PBE/OO/SZ, and PBE/OOwD2/SZ calculations although parallel displaced configurations (Fig. 3b) are also observed at smaller separations. Conversely, benzene molecules mainly arrange themselves in a parallel displaced configuration with PBE/DZP and PBE/TZP calculations resulting in large $g(r,\theta)$ estimates at low r and θ. This indicates that the structure of fluid can be successfully reproduced with a large basis set having orbital cutoff radius of 7.0 a.u., although a smaller radius OO/SZ calculation perform as well in capturing the overall coordination number and the detailed structure of the liquid.

Benzene has been shown to be nearly isotropic in the first solvation shell, with two anisotropic effects, i.e. parallel ordering at $r < 5$ Å and perpendicular ordering at $r > 5$ Å, almost canceling each other [25]. Therefore, the number of benzene molecules in the first solvation shell ($0 < r < 7.5$ Å), as well as at small ($0 < r < 5$ Å) and large separations (5 Å $< r < 6$ Å) within the first shell, is calculated as function of molecular orientations (Fig. 4) and compared to that of an isotropic liquid in the defined region. For PBE/SZ only, the r values are shifted by 1 Å due to a significant shift in COM-RDF values. In other words, total number of molecules are computed as a function of θ for molecular separations $0 < r < 6.5$ Å, $0 < r < 4$ Å, and 4 Å $< r < 5$ Å, for a better comparison of isotropy in the first shells. Unlike the experiments [25], the configurational distributions obtained in the first shell are anisotropic in all simulations (Fig. 4a). This is in accordance with the recent computational findings by Takeuchi et al. [77] and is attributed to the reduced perturbation effects induced by a small system size and lesser π–π interactions. At smaller molecular separations ($r < 5$ Å; $r < 4$ Å

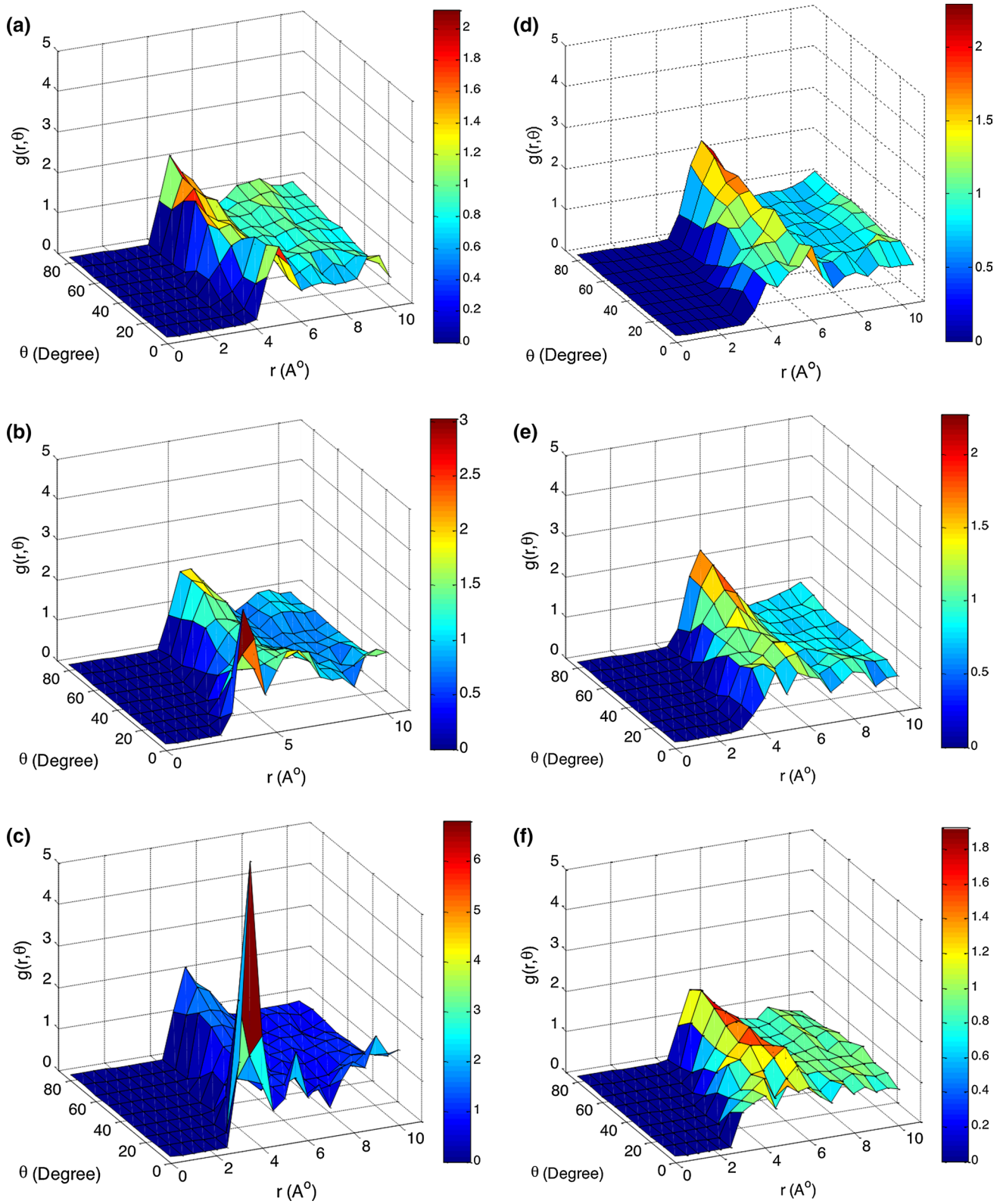

Fig. 2 Radial angular distribution functions for the COM of benzene molecules with **a** PBE/SZ, **b** PBE/DZP, **c** PBE/TZP, **d** PBE/DZP-7, **e** PBE/OO/SZ, **f** PBE/OOwD2/SZ. The radial and angular resolution is $\Delta r = 1$ Å, $\Delta\theta = 10°$ in (**d**), and $\Delta r = 0.5$ Å, $\Delta\theta = 10°$ in all other cases. PBE/DZP-7, PBE/SZ, PBE/OO/SZ, and PBE/OOwD2/SZ calculations show a higher preference for perpendicular molecular ordering, while PBE/DZP and PBE/TZP show a higher preference for parallel molecular arrangements. At small angles, PBE/DZP-7, PBE/OO/SZ, and PBE/OOwD2 have a shoulder next to main peak at $r \approx 4$ Å in accordance with ref [25] findings. The first peak is completely shifted to $r \approx 4$ Å with PBE/DZP and PBE/TZP

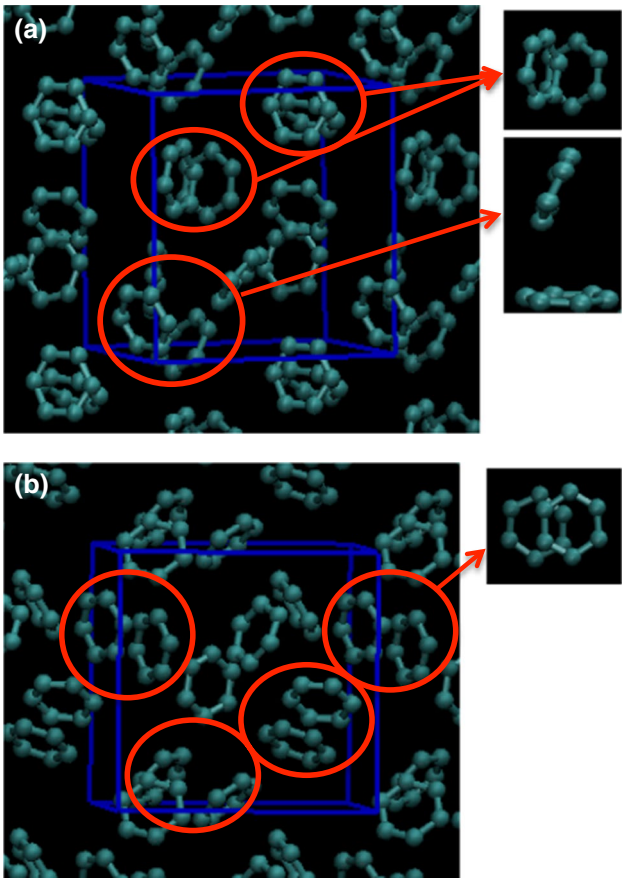

Fig. 3 **a** Perpendicular Y-shaped and distorted L-shaped ordering are the predominant geometry observed with PBE/DZP-7, PBE/SZ, PBE/OO/SZ, and PBE/OOwD2/SZ calculations. **b** Parallel displaced configuration is the predominant geometry observed with PBE/DZP and PBE/TZP calculations

for PBE/SZ), all simulations predict parallel arrangements (Fig. 4c). Profiles obtained by PBE/DZP-7, PBE/OO/SZ, and PBE/OOwD2/SZ are specifically in good agreement with Headen's findings [25]. PBE/DZP and PBE/TZP, on the other hand, show significantly higher preference for parallel displaced stacking and hence have the peak values exceeding the isotropic curve at much narrower angles ($\theta < 30°$). At larger separations within the first shell (Fig. 4e), only PBE/DZP, PBE/DZP-7, PBE/TZP, and PBE/OO/SZ show a small anisotropy toward perpendicular arrangement with the curves slightly exceeding the isotropic ones at angles $\theta > 65°$, $\theta > 85°$, $\theta > 80°$, and $\theta > 85°$, respectively. Although the number of molecules increases with increasing θ, calculated values are mainly lower than or in line with the isotropic estimates with PBE/OOwD2/SZ and PBE/SZ calculations.

Using the variationally optimized orbitals, the effect of simulation cell size on calculations was also investigated. An O(N) scheme based on a Krylov subspace method

Fig. 4 Number of benzene molecules as function of angle between ▶ aromatic planes **a** in the first coordination shell ($0 < r < 6.5$ Å for PBE/SZ and $0 < r < 7.5$ Å, for all others), **b** between $0 < r < 5$ Å ($0 < r < 4$ Å for PBE/SZ), and **d** between 5 Å $< r <$ 6 Å (4 Å $< r <$ 5 Å for PBE/SZ) are compared to the isotropic distributions within the defined region. Calculated distributions are compared with the experimental distributions reported by Headen et al. [25]. For the sake of simplicity, only the experimental isotropic distribution is given in (**a**) and (**b**), as the calculated curves are in general very similar to experimental findings. **c** Distributions of PBE/SZ given in graph **b** are enlarged for a better resolution and compared with the calculated isotropic distribution. **e** Distributions obtained for PBE/SZ, PBE/TZP, and PBE/OOwD2/SZ in graph **d** are enlarged for a better resolution and compared with the corresponding isotropic curves. The isotropic curves for PBE/OO/SZ and PBE/DZP-7 between 5 Å $< r <$ 6 Å (not shown) are overlapping with the isotropic curve of PBE/OOwD2/SZ given in (**e**). The best fit to the Headen et al. is obtained through PBE/DZP-7 and PBE/OO/SZ calculations

implemented in OpenMX [74] was used for the large system size. This scheme is ~6X faster than calculations with the O(N^3) direct diagonalization method (11 vs 68 s per MD step using 960 MPI processes with two threads per process). In addition, nearly the same C–C RDFs are obtained using both methods (Fig. 5a). We also compared $G(r)$ for a system containing 10 benzene molecules with a system of 80 benzene molecules. No significant difference in C–C RDF profiles is observed with different simulation cell size (Fig. 5b). Similarly, the first peak and the first minimum positions in COM-RDFs remain the same with large system PBE/OO/SZ (PBE/OO/SZ/80) calculations compared with small system calculations (Fig. 5c). However, a shift in the peak position by ~0.4 Å is observed with 80-benzene-molecule PBE/OOwD2/SZ simulations (PBE/OOwD2/SZ/80) compared to PBE/OOwD2/SZ calculations of 10 benzene molecules (Fig. 5c). The shift in the curve is attributed to an increase in attractive forces in the system.

Data presented so far reveal that simulations with a basis set constructed of variationally optimized numerical atomic orbitals yield radial structural properties in good general agreement with experiment and with results with larger basis sets. The detailed orientational structure of the fluid, as measured by $g(r,\theta)$, shows stronger dependence on the basis set than $G(r)$. In addition, the single zeta simulations are faster and hence computationally much cheaper. Using 120 MPI processors with two threads, computational times required for running one MD step to simulate 10 benzene molecules is 5.2, 13.7, 20.4, 32.4, 5.1, and 6.2 s with PBE/SZ, PBE/DZP, PBE/TZP, PBE/DZP-7, PBE/OO/SZ, and PBE/OOwD2/SZ, respectively. Similarly, using 960 MPI processors with two threads and employing the direct diagonalization method, the times needed to simulate one MD step of 80 benzene molecules is 346 and 68 s with PBE/DZP and PBE/OO/SZ, respectively.

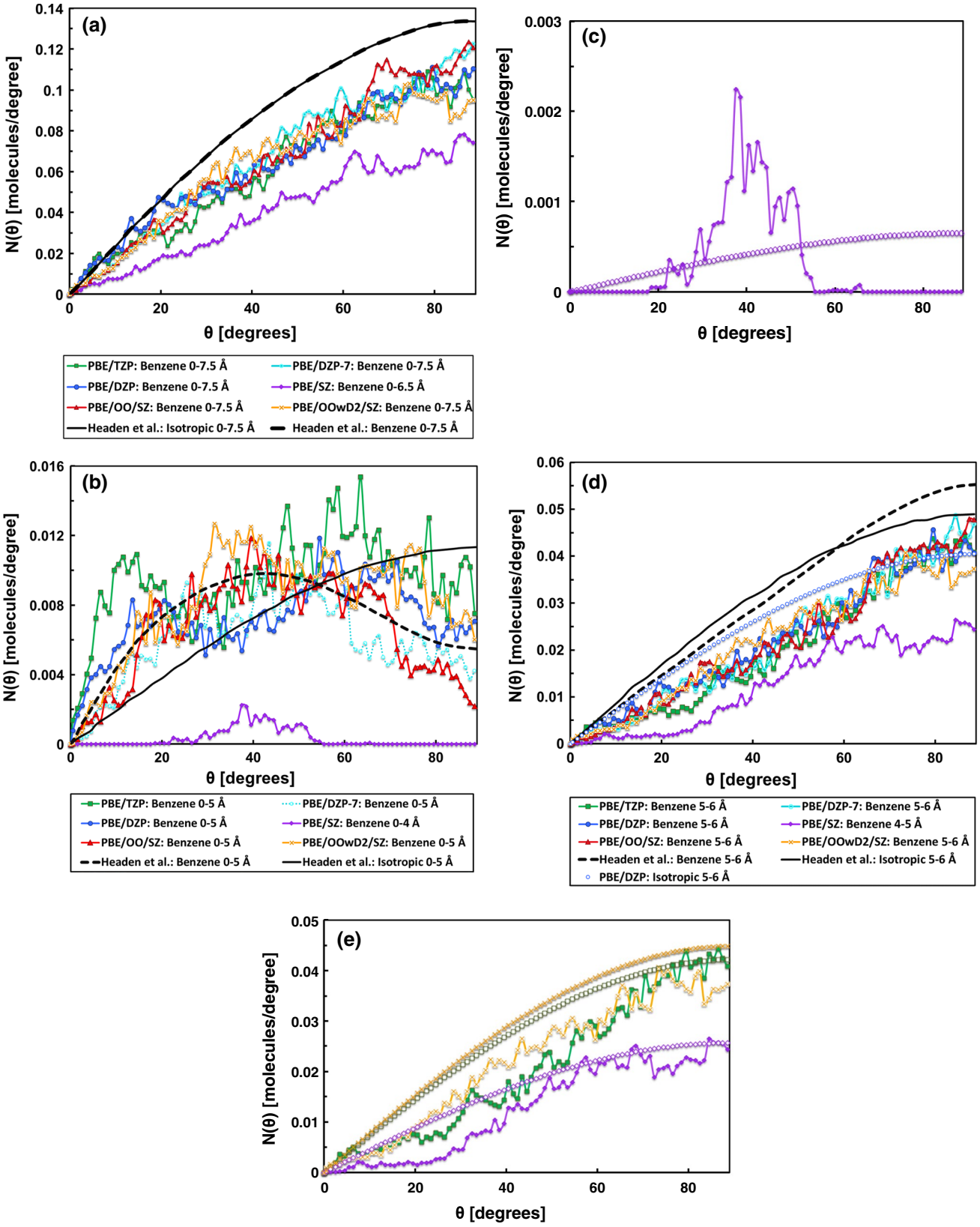
(a)
N(θ) [molecules/degree]
θ [degrees]
PBE/TZP: Benzene 0-7.5 Å
PBE/DZP-7: Benzene 0-7.5 Å
PBE/DZP: Benzene 0-7.5 Å
PBE/SZ: Benzene 0-6.5 Å
PBE/OO/SZ: Benzene 0-7.5 Å
PBE/OOwD2/SZ: Benzene 0-7.5 Å
Headen et al.: Isotropic 0-7.5 Å
Headen et al.: Benzene 0-7.5 Å
(c)
N(θ) [molecules/degree]
θ [degrees]
(b)
N(θ) [molecules/degree]
θ [degrees]
PBE/TZP: Benzene 0-5 Å
PBE/DZP-7: Benzene 0-5 Å
PBE/DZP: Benzene 0-5 Å
PBE/SZ: Benzene 0-4 Å
PBE/OO/SZ: Benzene 0-5 Å
PBE/OOwD2/SZ: Benzene 0-5 Å
Headen et al.: Benzene 0-5 Å
Headen et al.: Isotropic 0-5 Å
(d)
N(θ) [molecules/degree]
θ [degrees]
PBE/TZP: Benzene 5-6 Å
PBE/DZP-7: Benzene 5-6 Å
PBE/DZP: Benzene 5-6 Å
PBE/SZ: Benzene 4-5 Å
PBE/OO/SZ: Benzene 5-6 Å
PBE/OOwD2/SZ: Benzene 5-6 Å
Headen et al.: Benzene 5-6 Å
Headen et al.: Isotropic 5-6 Å
PBE/DZP: Isotropic 5-6 Å
(e)
N(θ) [molecules/degree]
θ [degrees]

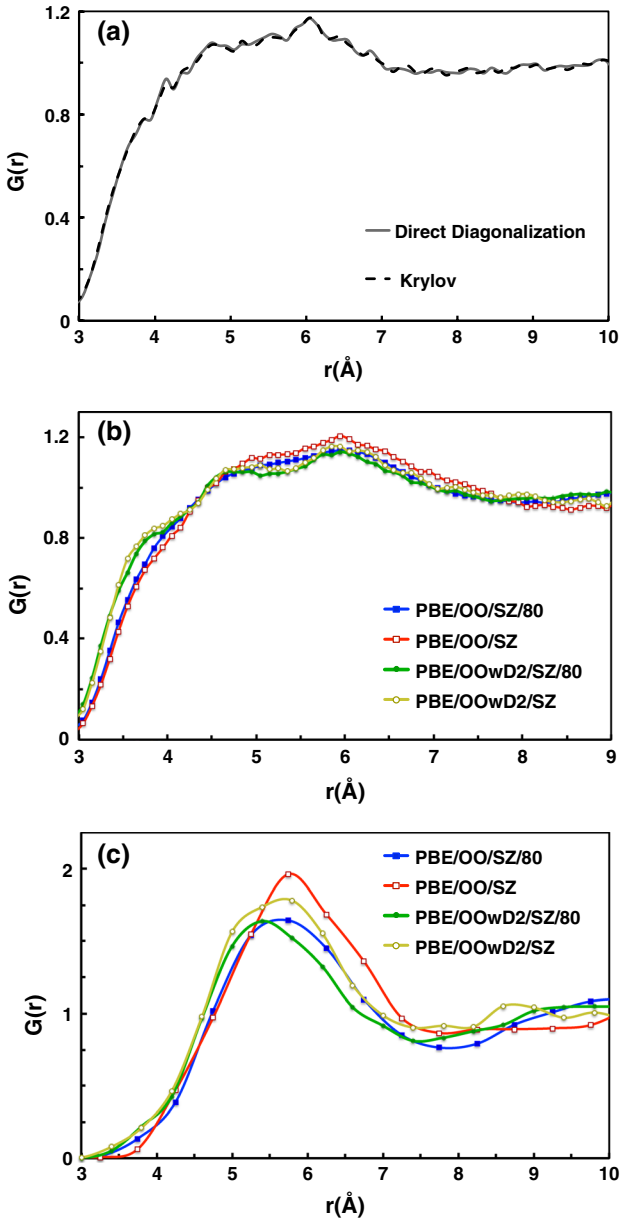

Fig. 5 **a** Comparison of the Krylov diagonalization method versus the direct diagonalization method. Intermolecular C–C pair distribution functions were obtained by 2-ps PBE/OO/SZ calculations in a system with 80 benzene molecules. **b** Intermolecular C–C pair distribution functions obtained with 80 benzene molecules versus 10 benzene molecules using variationally optimized orbitals (PBE/OO/SZ and PBE/OOwD2/SZ). **c** COM distribution functions obtained with 80 benzene molecules versus 10 benzene molecules using variationally optimized orbitals (PBE/OO/SZ and PBE/OOwD2/SZ). The COM $G(r)$ is more sensitive to system size than the C–C $G(r)$

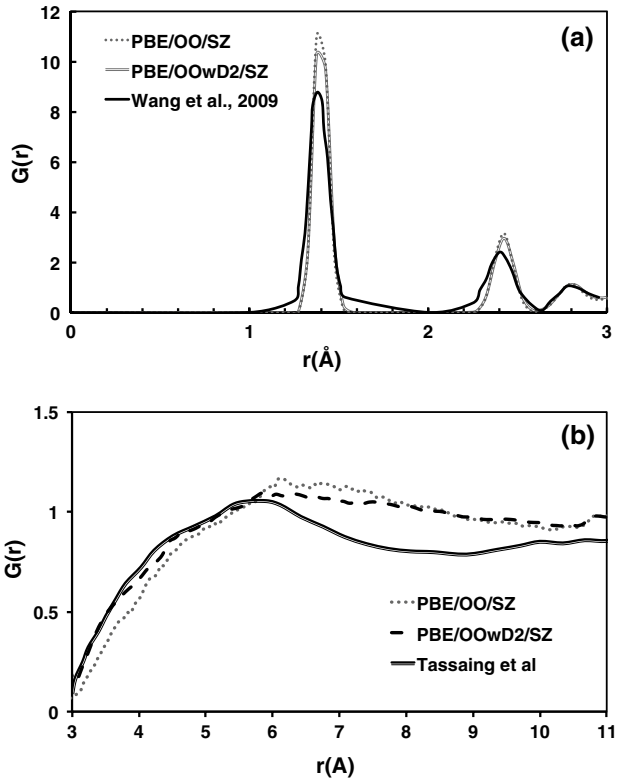

Fig. 6 Orbital optimization results in successful predictions under different conditions. **a** Intramolecular C–C pair distribution functions for benzene at 814 K and 1400 kg/m^3. Results of optimized orbital calculations are compared to the computational findings of Ref. [47]. **b** Intermolecular RDFs for supercritical benzene at 573 K and 570.2 kg/m^3. Results of optimized orbital calculations are compared to the experimental findings from Ref. [26]

It is also important to have a basis set that performs well under different environments to circumvent the need to develop several basis sets for each specific condition. Therefore, we have tested the transferability of variationally optimized orbitals at temperatures 573 K (density: 570.2 kg/m^3) and 814 K (density: 1,400 kg/m^3) and compared the results with the reported values (cf. Fig. 6). Figure 6a depicts the intramolecular C–C pair distribution functions for benzene at 814 K. Both PBE/OO/SZ and PBE/OOwD2/SZ have yielded in accurate predictions compared to Wang et al. findings where the phase transition in liquid benzene is studied by a detailed quantum MD simulation. The second peak is found to deviate <0.1 Å, whereas the first and third peaks exactly fit the first and third peak positions of Wang et al. [47]. Figure 6b, on the other hand, shows the intermolecular C–C pair RDF for supercritical benzene at 573 K. The profiles obtained by PBE/OO/SZ and PBE/OOwD2/SZ simulations are in good agreement with the calculated values by Tassaing et al. [26] especially at $r < 6$ Å. PBE/OOwD2/SZ better predicts the C–C $G(r)$ at ambient conditions (see Fig. 1b) than at supercritical conditions. The peak positions are calculated to be within 0.35 Å of Tassaing's results. Slightly higher $G(r)$ values are found at $r > 6$ Å with both cases compared to Tassaing's findings, which is attributed to the slight differences in system densities. Overall, optimized orbitals have good

transferability properties and yield in accurate results at different conditions.

4 Conclusions

First-principles MD simulations were performed to study the structure of liquid benzene. Variationally optimized numerical atomic orbitals based on the force theorem were used as a basis set in conjunction with the generic optimized orbitals. The accuracy of the simulations was compared with the recent experimental findings reported by Headen et al. based on neutron diffraction measurements. The local structure of benzene, with parallel displaced arrangements at small separations and Y-shaped geometry at larger separations, is successfully reproduced using basis sets with variationally optimized orbitals (PBE/OO/SZ and PBE/OOwD2/SZ). Among the simulations with the larger basis sets only calculations with double valence single polarization orbitals having a cutoff 7.0 a.u demonstrated matching local structure. The smaller basis set size has substantially increased the simulation speed by at least a factor of 2–6 compared to a larger basis set of generic orbitals. Yet, the accuracy is significantly improved or at least preserved compared to the accuracy of the same size or a larger basis set formed by generic orbitals, respectively. PBE/OO/SZ is found to predict the local ordering in benzene slightly better than PBE/OOwD2/SZ, while PBE/OOwD2/SZ is observed to yield in better C–C RDF profiles. The order-N Krylov technique is found to perform well for molecular liquids, with only a factor of 2 increase in the wall time per simulation step between a 120 and 960 atom system. The transferability of the variationally optimized orbitals is also explored under different environmental conditions and shown to result in accurate predictions at different conditions. Overall, DFT simulations using orbital optimization are shown to be efficient and accurate in predicting the structure of molecular liquid benzene. Further studies will assess the applicability of simulation methodology employed here, using order-N DFT methods and compact optimized basis functions, to the study of condensed phase chemical reactivity.

Acknowledgments This work was performed under the auspices of the U.S. Department of Energy by Lawrence Livermore National Laboratory under Contract DE-AC52-07NA27344. Laurence E. Fried thanks Prof. Gregory S. Ezra for his patient encouragement and guidance at Cornell University.

References

1. Vallee R et al (2000) Nonlinear optical properties and crystalline orientation of 2-methyl-4-nitroaniline layers grown on nanostructured poly(tetrafluoroethylene) substrates. J Am Chem Soc 122(28):6701–6709
2. Meyer EA, Castellano RK, Diederich F (2003) Interactions with aromatic rings in chemical and biological recognition. Angew Chem Int Ed 42(11):1210–1250
3. Baker CM, Grant GH (2007) Role of aromatic amino acids in protein–nucleic acid recognition. Biopolymers 85(5–6):456–470
4. Hunter CA (1993) Aromatic interactions in proteins, DNA and synthetic receptors. Philos Trans R Soc Mathe Phys Eng Sci 345(1674):77–85
5. Cox EG, Smith JAS (1954) Crystal structure of benzene at-3-degrees-C. Nature 173(4393):75
6. Cox EG, Cruickshank DWJ, Smith JAS (1955) Crystal structure of benzene—new type of systematic error in precision X-ray crystal analysis. Nature 175(4461):766
7. Cox EG, Cruickshank DWJ, Smith JAS (1958) The crystal structure of benzene at-3-degrees-C. Proc R Soc Lond Ser Mathe Phys Sci 247(1248):1–21
8. Janda KC et al (1975) Benzene dimer—polar molecule. J Chem Phys 63(4):1419–1421
9. Steed JM, Dixon TA, Klemperer W (1979) Molecular-beam studies of benzene dimer, hexafluorobenzene dimer and benzene–hexafluorobenzene. J Chem Phys 70(11):4940–4946
10. Hopkins JB, Powers DE, Smalley RE (1981) Mass-selective 2-color photo-ionization of benzene clusters. J Phys Chem 85(25):3739–3742
11. Langridgesmith PRR et al (1981) Ultraviolet-spectra of benzene clusters. J Phys Chem 85(25):3742–3746
12. Venturo VA, Felker PM (1993) Intermolecular Raman bands in the ground-state of benzene dimer. J Chem Phys 99(1):748–751
13. Hobza P, Selzle HL, Schlag EW (1996) Potential energy surface for the benzene dimer. Results of ab initio CCSD(T) calculations show two nearly isoenergetic structures: T-shaped and parallel-displaced. J Phys Chem 100(48):18790–18794
14. Sato T, Tsuneda T, Hirao K (2005) A density-functional study on pi-aromatic interaction: benzene dimer and naphthalene dimer. J Chem Phys 123(10):104307
15. Sinnokrot MO, Sherrill CD (2006) High-accuracy quantum mechanical studies of pi–pi interactions in benzene dimers. J Phys Chem A 110(37):10656–10668
16. van der Avoird A et al (2010) Vibration–rotation–tunneling states of the benzene dimer: an ab initio study. Phys Chem Chem Phys 12(29):8219–8240
17. Henson BF et al (1992) Raman-vibronic double-resonance spectroscopy of benzene dimer isotopomers. J Chem Phys 97(4):2189–2208
18. Erlekam U et al (2006) An experimental value for the B-1u C–H stretch mode in benzene. J Chem Phys 124(17):171101
19. Tsuzuki S et al (2005) Ab initio calculations of structures and interaction energies of toluene dimers including CCSD(T) level electron correlation correction. J Chem Phys 122(14):144323
20. Lowden LJ, Chandler D (1974) Theory of intermolecular pair correlations for molecular liquids—applications to liquids carbon-tetrachloride, carbon-disulfide, carbon diselenide, and benzene. J Chem Phys 61(12):5228–5241
21. Narten AH (1968) Diffraction pattern and structure of liquid benzene. J Chem Phys 48(4):1630–1634
22. Narten AH (1977) X-ray-diffraction pattern and models of liquid benzene. J Chem Phys 67(5):2102–2108
23. Katayama M et al (2010) Liquid structure of benzene and its derivatives as studied by means of X-ray scattering. Phys Chem Liq 48(6):797–809
24. Bartsch E et al (1985) A neutron and X-ray-diffraction study of the binary-liquid aromatic system benzene-hexafluorobenzene.1. The pure components. Ber Bunsen Ges Phys Chem Chem Phys 89(2):147–156

25. Headen TF et al (2010) Structure of pi–pi interactions in aromatic liquids. J Am Chem Soc 132(16):5735–5742
26. Tassaing T et al (2000) The structure of liquid and supercritical benzene as studied by neutron diffraction and molecular dynamics. J Chem Phys 113(9):3757–3765
27. Misawa M, Fukunaga T (1990) Structure of liquid benzene and naphthalene studied by pulsed neutron total scattering. J Chem Phys 93(5):3495–3502
28. Fu C-F, Tian SX (2011) A comparative study for molecular dynamics simulations of liquid benzene. J Chem Theory Comput 7(7):2240–2252
29. Bogdan TV (2006) Atom-atomic potentials and the correlation distribution functions for modeling liquid benzene by the molecular dynamics methods. Russ J Phys Chem 80:S14–S20
30. Chelli R et al (2001) The fast dynamics of benzene in the liquid phase—Part II. A molecular dynamics simulation. Phys Chem Chem Phys 3(14):2803–2810
31. Baker CM, Grant GH (2006) The structure of liquid benzene. J Chem Theory Comput 2(4):947–955
32. Coutinho K, Canuto S, Zerner MC (1997) Calculation of the absorption spectrum of benzene in condensed phase. A study of the solvent effects. Int J Quantum Chem 65(5):885–891
33. Jorgensen WL et al (1993) Monte-Carlo simulations of pure liquid substituted benzenes with OPLS potential functions. J Comput Chem 14(2):206–215
34. Cabaco MI et al (1997) Neutron diffraction and molecular dynamics study of liquid benzene and its fluorinated derivatives as a function of temperature. J Phys Chem B 101(35):6977–6987
35. Hunter CA, Sanders JKM (1990) The nature of pi–pi interactions. J Am Chem Soc 112(14):5525–5534
36. Righini R (1993) Ultrafast optical kerr-effect in liquids and solids. Science 262(5138):1386–1390
37. Zorkii PM, Lanshina LV, Bogdan TV (2008) Computer simulation and diffraction studies of the structure of liquid benzene. J Struct Chem 49(3):524–547
38. Forsman J, Woodward CE, Trulsson M (2011) A classical density functional theory of ionic liquids. J Phys Chem B 115(16):4606–4612
39. Song Z, Wang H, Xing L (2009) Density functional theory study of the ionic liquid [emim]OH and complexes [emim]OH(H2O) n (n = 1,2). J Solut Chem 38(9):1139–1154
40. Umebayashi Y et al (2009) Raman spectroscopic study, DFT calculations and MD simulations on the conformational isomerism of N-Alkyl-N-methylpyrrolidinium Bis-(trifluoromethanesulfonyl) amide ionic liquids. J Phys Chem B 113(13):4338–4346
41. Waller MP et al (2006) Hybrid density functional theory for pi-stacking interactions: application to benzenes, pyridines, and DNA bases. J Comput Chem 27(4):491–504
42. Yan Z, Truhlar DG (2005) How well can new-generation density functional methods describe stacking interactions in biological systems? Phys Chem Chem Phys 7(14):2701–2705
43. Tachikawa H (2013) Double pi-pi stacking dynamics of benzene trimer cation: direct ab initio molecular dynamics (AIMD) study. Theor Chem Acc 132(7):1374
44. Sherrill CD, Takatani T, Hohenstein EG (2009) An assessment of theoretical methods for nonbonded interactions: comparison to complete basis set limit coupled-cluster potential energy curves for the benzene dimer, the methane dimer, benzene-methane, and benzene-H2S. J Phys Chem A 113(38):10146–10159
45. Pitonak M et al (2008) Benzene dimer: high-level wave function and density functional theory calculations. J Chem Theory Comput 4(11):1829–1834
46. Wen X-D, Hoffmann R, Ashcroft NW (2011) Benzene under high pressure: a story of molecular crystals transforming to saturated networks, with a possible intermediate metallic phase. J Am Chem Soc 133(23):9023–9035
47. Wang C, Zhang P (2010) The equation of state and nonmetal–metal transition of benzene under shock compression. J Appl Phys 107(8):083502
48. Goldman N et al (2005) Bonding in the superionic phase of water. Phys Rev Lett 94(21):217801
49. Schwegler E et al (2008) Melting of ice under pressure. Proc Natl Acad Sci U S A 105(39):14779–14783
50. Ozaki T (2003) Variationally optimized atomic orbitals for large-scale electronic structures. Phys Rev B 67(15):155108
51. Ozaki T, Kino H (2004) Numerical atomic basis orbitals from H to Kr. Phys Rev B 69(19):195113
52. Junquera J et al (2001) Numerical atomic orbitals for linear-scaling calculations. Phys Rev B 64(23):235111
53. Corsetti F et al (2013) Optimal finite-range atomic basis sets for liquid water and ice. J Phys: Condens Matter 25(43):435504
54. Ozaki T, Kino H (2004) Variationally optimized basis orbitals for biological molecules. J Chem Phys 121(22):10879–10888
55. Ohwaki T et al (2012) Large-scale first-principles molecular dynamics for electrochemical systems with O(N) methods. J Chem Phys 136(13):134101
56. Jorgensen WL, Tiradorives J (1988) The OPLS potential functions for proteins—energy minimizations for crystals of cyclic-peptides and crambin. J Am Chem Soc 110(6):1657–1666
57. Jorgensen WL, Severance DL (1990) Aromatic aromatic interactions—free-energy profiles for the benzene dimer in water, chloroform, and liquid benzene. J Am Chem Soc 112(12):4768–4774
58. Van der Spoel D et al (2005) GROMACS: fast, flexible, and free. J Comput Chem 26(16):1701–1718
59. Hess B (2009) GROMACS 4: algorithms for highly efficient, load-balanced, and scalable molecular simulation. Abstracts of Papers of the American Chemical Society 237
60. NISTChemistryWebBook. http://webbook.nist.gov/chemistry
61. Nose S (1984) A molecular-dynamics method for simulations in the canonical ensemble. Mol Phys 52(2):255–268
62. Hoover WG (1985) Canonical dynamics—equilibrium phase-space distributions. Phys Rev A 31(3):1695–1697
63. Parrinello M, Rahman A (1981) Polymorphic transitions in single-crystals—a new molecular-dynamics method. J Appl Phys 52(12):7182–7190
64. Nose S, Klein ML (1983) Constant pressure molecular-dynamics for molecular-systems. Mol Phys 50(5):1055–1076
65. Hess B et al (1997) LINCS: a linear constraint solver for molecular simulations. J Comput Chem 18(12):1463–1472
66. Hess B (2008) P-LINCS: a parallel linear constraint solver for molecular simulation. J Chem Theory Comput 4(1):116–122
67. Ozaki T, Kino H (2005) Efficient projector expansion for the ab initio LCAO method. Phys Rev B 72(4):045121
68. OpenMX. http://www.openmx-square.org/
69. Hohenberg P, Kohn W (1964) Inhomogeneous electron gas. Phys Rev B 136(3B):B864
70. Perdew JP, Burke K, Ernzerhof M (1996) Generalized gradient approximation made simple. Phys Rev Lett 77(18):3865–3868
71. Morrison I, Bylander DM, Kleinman L (1993) Nonlocal hermitian norm-conserving vanderbilt pseudopotential. Phys Rev B 47(11):6728–6731
72. Grimme S (2006) Semiempirical GGA-type density functional constructed with a long-range dispersion correction. J Comput Chem 27(15):1787–1799
73. Soler JM et al (2002) The SIESTA method for ab initio order-N materials simulation. J Phys: Condens Matter 14(11):2745–2779
74. Ozaki T (2006) O(N) Krylov-subspace method for large-scale ab initio electronic structure calculations. Physical Review B 74(24):245101

75. Woodcock LV (1971) Isothermal molecular dynamics calculations for liquid salts. Chem Phys Lett 10(3):257–261
76. Nose S (1984) A unified formulation of the constant temperature molecular-dynamics methods. J Chem Phys 81(1):511–519
77. Takeuchi H (2012) Structural features of small benzene clusters (C6H6)(n) (n <= 30) as investigated with the All-Atom OPLS potential. J Phys Chem A 116(41):10172–10181